

Alkaline-Earth Metal Mercury Intermetallics $A_{11-x}Hg_{54+x}$ ($A = Ca, Sr$)

Andriy V. Tkachuk and Arthur Mar*

Department of Chemistry, University of Alberta, Edmonton, Alberta, Canada T6G 2G2

Received July 30, 2007

Re-examination of the mercury-rich regions of the Ca–Hg and Sr–Hg phase diagrams has shown that the phases previously identified as “AHg_{3.6}” should be reformulated as $A_{11-x}Hg_{54+x}$ ($A = Ca, Sr$). The crystal structures for representative members of these $A_{11-x}Hg_{54+x}$ phases were determined from single-crystal X-ray diffraction data (Pearson symbol *hP65*, space group *P6̄*; $a = 13.389(1) \text{ \AA}$, $c = 9.615(1) \text{ \AA}$ for $Ca_{10.92(2)}Hg_{54.08}$ ($x = 0.08(2)$); $a = 13.602(2) \text{ \AA}$, $c = 9.818(1) \text{ \AA}$ for $Sr_{10.48(4)}Hg_{54.52}$ ($x = 0.52(4)$)) and confirmed by powder Rietveld refinements ($R_B = 0.020$ for $Ca_{10.7(2)}Hg_{54.3}$ and 0.014 for $Sr_{10.7(3)}Hg_{54.3}$). Diverse coordination polyhedra surround the A (CN14–16, multiply capped pentagonal or hexagonal prisms as well as Friauf polyhedra) and Hg atoms (CN11–13, pentacapped trigonal prisms and icosahedra). Partial disorder of Hg into one of the A sites accounts for the nonstoichiometry in the $A_{11-x}Hg_{54+x}$ phases. If this disordered A site is completely occupied by Hg atoms, the composition is constrained to a maximum of $x = 2$ in $A_{11-x}Hg_{54+x}$, corresponding to a small homogeneity range of “ $A_{0.14-0.17}Hg_{0.86-0.83}$ ”; the true homogeneity range is likely narrower. The structure can be regarded as being built up from a stacking of triangular nets with hexagonal voids that are filled with single atoms or various clusters. In particular, the presence of triangular Hg₃ clusters in ordered orientations distinguishes this structure from that of the related Gd₁₄Ag₅₁-type structure, in which triangular Ag₃ clusters are in disordered orientations. Band structure calculations reveal a small degree of electron transfer from the A to Hg atoms, supporting the presence of a partially anionic mercuride substructure.

Introduction

Although alloys of mercury (“amalgams”) have been known since antiquity, many of their structures and phase relations remain poorly understood. In combination with highly electropositive metals such as alkali metals, partial electron transfer to Hg atoms may occur, resulting in some ionic bonding character and formation of anionic “mercuride” substructures.¹ These alkali metal amalgams possess structures that can be very complex, especially for the Hg-rich phases. Structure determination is also hampered by the extreme air sensitivity of these compounds. Relatively less is known about the alkaline-earth metal amalgams, which have not been investigated as thoroughly. In the Hg-rich regions of the Ca–Hg and Sr–Hg phase diagrams,^{2,3} the incongruently melting phases “ $A_{14}Hg_{51}$ ” ($A = Ca, Sr$) (or “AHg_{3.6}” as originally reported) were previously identified. The compositions of these phases were not directly deter-

mined but were assumed on the basis of the similarity of their powder X-ray diffraction patterns to that of the hexagonal Gd₁₄Ag₅₁-type structure,⁴ in which triangular Ag₃ clusters are in disordered orientations near the origin of the unit cell. Although this structure type has been assigned to many other phases with the formulation $M_{14}X_{51}$ ($M = Ca, Sr, RE, U, Th, Pu, Zr, Hf$; $X = Cu, Ag, Au, Cd, Hg$)^{5–22} on

* To whom correspondence should be addressed. E-mail: arthur.mar@ualberta.ca.

(1) Deiseroth, H. J. *Prog. Solid State Chem.* **1997**, *25*, 73–123.
 (2) Bruzzone, G.; Merlo, F. *J. Less-Common Met.* **1973**, *32*, 237–241.
 (3) Bruzzone, G.; Merlo, F. *J. Less-Common Met.* **1974**, *35*, 153–157.

(4) Bailey, D. M.; Kline, G. R. *Acta Crystallogr. Sect. B* **1971**, *27*, 650–653.

(5) Runnalls, O. J. C. *Can. J. Chem.* **1956**, *34*, 133–145.

(6) Köster, W.; Meixner, J. *Z. Metallkd.* **1965**, *56*, 695–703.

(7) Steeb, S.; Godel, D.; Löhr, C. *J. Less-Common Met.* **1968**, *15*, 137–141.

(8) Donolato, C.; Steeb, S. *J. Less-Common Met.* **1969**, *18*, 312–313.

(9) McMasters, O. D.; Gschneidner, K. A., Jr.; Venteicher, R. F. *Acta Crystallogr. Sect. B* **1970**, *26*, 1224–1229.

(10) McMasters, O. D.; Gschneidner, K. A., Jr.; Bruzzone, G.; Palenzona, A. *J. Less-Common Met.* **1971**, *25*, 135–160.

(11) Palenzona, A. *J. Less-Common Met.* **1971**, *25*, 367–372.

(12) Berlin, B. *J. Less-Common Met.* **1972**, *29*, 337–348.

(13) Bailey, D. M. *J. Less-Common Met.* **1973**, *30*, 164–166.

(14) Bruzzone, G.; Fornasini, M. L.; Merlo, F. *J. Less-Common Met.* **1973**, *30*, 361–375.

(15) Gabathuler, J.-P.; White, P.; Parthé, E. *Acta Crystallogr. Sect. B* **1975**, *31*, 608–610.

(16) Merlo, F.; Fornasini, M. L. *J. Less-Common Met.* **1979**, *64*, 221–231.

Table 1. Models in Refinement of $A_{11-x}\text{Hg}_{54+x}$ ($A = \text{Ca}, \text{Sr}$)

model	$\text{Ca}_{11-x}\text{Hg}_{54+x}$			$\text{Sr}_{11-x}\text{Hg}_{54+x}$		
	A	B	C	A	B	C
contents of site $2h$ ($1/3, 2/3, z$)	1.00 Ca	0.25(1) Hg	0.96(1) Ca/0.04 Hg	1.00 Sr	0.58(1) Hg	0.74(2) Sr/0.26 Hg
U_{eq} (\AA^2) for site $2h$	0.001(1)	0.013(2)	0.008(2)	0.002(1)	0.018(1)	0.016(1)
formula	$\text{Ca}_{11}\text{Hg}_{54}$	$\text{Ca}_9\text{Hg}_{54.5}$	$\text{Ca}_{10.9}\text{Hg}_{54.1}$	$\text{Sr}_{11}\text{Hg}_{54}$	$\text{Sr}_9\text{Hg}_{55.2}$	$\text{Sr}_{10.5}\text{Hg}_{54.5}$
R_1/wR_2	0.044/0.106	0.044/0.105	0.044/0.105	0.064/0.172	0.063/0.169	0.063/0.169

the basis of powder X-ray diffraction, it has only been verified by single-crystal X-ray diffraction in only two instances: $\text{Gd}_{14}\text{Ag}_{51}$ itself and $\text{Hf}_{14}\text{Cu}_{51}$.^{4,15}

In this work, we have re-examined the structure of these $A_{14}\text{Hg}_{51}$ ($A = \text{Ca}, \text{Sr}$) phases and assert that their true composition should be $A_{11-x}\text{Hg}_{54+x}$. The revised structure exhibits, among other differences, triangular Hg_3 clusters now arranged in ordered orientations. A band structure calculation was performed to evaluate the degree of electron transfer, if any, to the Hg atoms.

Experimental Section

Synthesis. Because of the extreme sensitivity of the reagents and products to air and moisture, all procedures were performed under argon in a glovebox. A 0.3-g mixture of the elements (Ca or Sr dendritic pieces, 99.99%; Hg, 99.9999%; all from Aldrich) was placed in a Nb container, which was arc-welded under argon and then sealed within a fused-silica tube under vacuum. Stoichiometries investigated were $A_{0.10}\text{Hg}_{0.90}$, $A_{0.15}\text{Hg}_{0.85}$, $A_{0.20}\text{Hg}_{0.80}$, and $A_{0.25}\text{Hg}_{0.75}$. The mixtures were heated at 400 °C for 2 d, slowly cooled at 0.6 °C/h to 200 °C, held there for 1 month, and then quenched in cold water. The products were characterized by powder X-ray diffraction on an Inel powder X-ray diffractometer (Cu $K\alpha_1$ radiation) equipped with a curved position-sensitive (CPS) 120 detector. Crystals of the title compounds used for the structure determinations were extracted from the reactions with nominal stoichiometry $A_{0.15}\text{Hg}_{0.85}$. Samples of $A_{11-x}\text{Hg}_{54+x}$ oxidize immediately upon exposure to air and moisture and decompose completely within a few days when stored under oil.

Structure Determination. Single crystals were selected from the products and mounted on a glass fiber under Paratone-N oil. Single-crystal X-ray diffraction data were collected on a Bruker Platform/SMART 1000 CCD diffractometer at -80 °C using ω scans. Structure solution and refinement were carried out with use of the SHELXTL (version 6.12) program package.²³ Because of the very high absorption coefficients and very low transmission factors (e.g., $\mu(\text{Mo } K\alpha) = 141.20 \text{ mm}^{-1}$ and transmission factors = 0.00–0.02 for $\text{Sr}_{10.5}\text{Hg}_{54.5}$), face-indexed numerical absorption corrections were important. The intensity data revealed Laue symmetry $6/m$ and no systematic absences, consistent with the possible hexagonal space groups $P6$, $P\bar{6}$, and $P6/m$. When an initial model was chosen in space group $P6/m$ based on $\text{Gd}_{14}\text{Ag}_{51}$, attempts to refine the structure failed. Structure solution by direct methods and refinement could only proceed successfully in space group $P\bar{6}$.

All sites could be assigned in a straightforward manner except for the one at $2h$ ($1/3, 2/3, \sim 0.19$). Several models were examined, as summarized in Table 1. If this site was occupied fully by Ca or Sr atoms only, the displacement parameters were too small (0.001(1) or 0.002(1) \AA^2), implying the presence of greater electron density. If this site was allowed to be partially occupied by Hg atoms only, the displacement parameters became reasonable (0.013(2) or 0.018(1) \AA^2). However, this model has two problems. First, the distances to this site (3.2–3.8 \AA) are somewhat longer than the Hg–Hg distances (2.9 to ~ 3.5 \AA) associated with the other Hg sites, so that larger A atoms could feasibly occupy this site as well. Second, partial occupancy of this site implies the presence of vacancies with a large volume in the structure, an unlikely situation for intermetallic structures, which are typically densely packed. Thus, this site was allowed to be fully occupied by a mixture of A and Hg atoms. The refined occupancies converged to 0.96(1) Ca/0.04 Hg and 0.74(2) Sr/0.26 Hg, indicating a site preference for alkaline-earth metal atoms. Crystal data and further details of the data collections are given in Table 2.

Powder X-ray diffraction data, collected on samples sealed between two pieces of tape under argon atmosphere, were also refined with the full-profile Rietveld method using the program LHPM-Rietica.²⁴ Initial positions were taken from the single-crystal structures determined above. The final cycles of least-squares refinement included scale factor, background, zero point, cell parameters, pseudo-Voigt peak profile parameters, occupancy, and atomic coordinates. The results obtained here from powder data validate those from the single-crystal data above. Further details (Table S1), including fits of the Rietveld refinement results to the powder patterns (Figure S1), are relegated to the Supporting Information.

Atomic positions were standardized with the program STRUCTURE TIDY.²⁵ Final values of the positional and displacement parameters are given in Table 3. Interatomic distances less than 4.0 \AA are listed in Tables S2 and S3 (Supporting Information), and a condensed listing of ranges of interatomic distances is given in Table 4. Further data, in the form of crystallographic information files (CIFs) are available as Supporting Information or may be obtained from Fachinformationszentrum Karlsruhe, Abt. PROKA, 76344 Eggenstein-Leopoldshafen, Germany (No. CSD-419016 and 419017).

Band Structure. A tight-binding linear muffin tin orbital (TB-LMTO) band structure calculation was performed on an idealized $\text{Ca}_{11}\text{Hg}_{54}$ structure within the local density and atomic spheres approximations using the Stuttgart TB-LMTO program.²⁶ The basis sets consisted of Ca 4s/4p/3d and Hg 6s/6p/6d/5f orbitals, with the Ca 4p and Hg 5f orbitals being downfolded. Integrations

(17) Palenzona, A.; Cirafici, S. *J. Less-Common Met.* **1986**, *124*, 245–249.

(18) Cirafici, S.; Palenzona, A. *J. Less-Common Met.* **1987**, *135*, 1–4.

(19) Dommann, A.; Hulliger, F. *J. Less-Common Met.* **1988**, *141*, 261–273.

(20) Palenzona, A.; Cirafici, S. *J. Less-Common Met.* **1988**, *143*, 167–171.

(21) Dommann, A.; Ott, H. R.; Hulliger, F.; Fischer, P. *J. Less-Common Met.* **1990**, *160*, 171–180.

(22) Canepa, F.; Palenzona, A.; Eggenhöfner, R. *Physica B* **1992**, *176*, 293–300.

(23) Sheldrick, G. M. *SHELXTL*, version 6.12; Bruker AXS Inc.: Madison, WI, 2001.

(24) Hunter, B. LHPM-Rietica, version 1.7.7. *International Union of Crystallography Commission on Powder Diffraction Newsletter* **1998**, (20); (www.rietica.org).

(25) Gelato, L. M.; Parthé, E. *J. Appl. Crystallogr.* **1987**, *20*, 139–143.

(26) Tank, R.; Jepsen, O.; Burkhardt, A.; Andersen, O. K. *TB-LMTO-ASA program*, version 4.7; Max Planck Institut für Festkörperforschung: Stuttgart, 1998.

Table 2. Crystallographic Data for $A_{11-x}\text{Hg}_{54+x}$ ($A = \text{Ca}, \text{Sr}$)

formula	$\text{Ca}_{10.92(2)}\text{Hg}_{54.08}$	$\text{Sr}_{10.48(4)}\text{Hg}_{54.52}$
formula mass (amu)	11285.58	11854.42
space group	$P\bar{6}$ (no. 174)	$P\bar{6}$ (no. 174)
T (°C)	−80	−80
a (Å)	13.389(1)	13.602(2)
c (Å)	9.615(1)	9.818(1)
V (Å ³)	1492.8(3)	1573.0(3)
Z	1	1
ρ_{calcd} (g cm ^{−3})	12.554	12.514
radiation	Mo $K\alpha$, $\lambda = 0.71073$ Å	Mo $K\alpha$, $\lambda = 0.71073$ Å
μ (mm ^{−1})	139.33	141.20
2θ range	3.52–60.98°	3.46–61.02°
no. of data collected	16837 ($R_{\text{int}} = 0.124$)	18788 ($R_{\text{int}} = 0.157$)
no. of unique data	3219 (2966 with $F^2 > 2\sigma(F^2)$)	3388 (2732 with $F^2 > 2\sigma(F^2)$)
no. of variables	113	113
$R(F)$ ($F^2 > 2\sigma(F^2)$) ^a	0.044	0.063
$R_w(F^2)$ ^b	0.105	0.169
goodness of fit	1.039	1.010

$$^a R(F) = \frac{\sum |F_o| - |F_c|}{\sum |F_o|}, \quad ^b R_w(F^2) = \frac{[\sum (w(F_o^2 - F_c^2))^2] / \sum w F_o^4}{1/2}, \quad w^{-1} = [\sigma^2(F_o^2) + (Ap)^2 + Bp], \quad \text{where } p = [\max(F_o^2, 0) + 2F^2]/3.$$

Table 3. Positional and Equivalent Isotropic Displacement Parameters for $A_{11-x}\text{Hg}_{54+x}$ ($A = \text{Ca}, \text{Sr}$)

atom	Wyckoff position	$\text{Ca}_{10.92(2)}\text{Hg}_{54.08}$				$\text{Sr}_{10.48(4)}\text{Hg}_{54.52}$			
		x	y	z	U_{eq} (Å ²) ^a	x	y	z	U_{eq} (Å ²) ^a
A1	3k	0.4648(6)	0.0570(6)	½	0.0083(12)	0.4601(4)	0.0520(5)	½	0.0132(9)
A2	3k	0.2095(6)	0.2581(6)	½	0.0080(12)	0.2035(4)	0.2542(4)	½	0.0122(9)
A3	3j	0.4314(6)	0.3094(6)	0	0.0066(11)	0.4325(4)	0.3082(4)	0	0.0110(9)
A4 ^b	2h	1/3	2/3	0.1958(7)	0.008(2)	1/3	2/3	0.1922(5)	0.016(1)
Hg1	6l	0.4502(1)	0.2780(1)	0.3450(1)	0.0097(2)	0.4493(1)	0.2772(1)	0.3462(2)	0.0153(3)
Hg2	6l	0.2376(1)	0.0488(1)	0.3442(1)	0.0147(2)	0.2378(1)	0.0509(1)	0.3374(2)	0.0205(3)
Hg3	6l	0.1796(1)	0.2044(1)	0.1713(1)	0.0141(2)	0.1752(2)	0.2010(1)	0.1666(2)	0.0193(3)
Hg4	6l	0.4599(1)	0.1054(1)	0.1623(1)	0.0104(2)	0.4601(1)	0.1044(1)	0.1623(2)	0.0166(3)
Hg5	6l	0.1409(1)	0.4149(1)	0.2958(1)	0.0128(2)	0.1389(2)	0.4116(2)	0.2837(2)	0.0229(4)
Hg6	6l	0.3940(1)	0.4490(1)	0.2616(1)	0.0097(2)	0.3895(1)	0.4473(1)	0.2618(2)	0.0163(3)
Hg7	3k	0.3460(1)	0.5470(1)	½	0.0134(3)	0.3339(2)	0.5416(2)	½	0.0222(5)
Hg8	3j	0.2364(1)	0.0279(1)	0	0.0153(3)	0.2360(2)	0.0247(2)	0	0.0209(5)
Hg9	3j	0.2494(1)	0.4137(1)	0	0.0131(3)	0.2476(2)	0.4136(2)	0	0.0195(4)
Hg10	3j	0.1060(1)	0.5100(1)	0	0.0114(2)	0.1024(2)	0.5090(2)	0	0.0190(4)
Hg11	2i	2/3	1/3	0.1568(2)	0.0122(3)	2/3	1/3	0.1647(3)	0.0173(5)
Hg12	2g	0	0	0.3448(2)	0.0129(3)	0	0	0.3435(3)	0.0164(5)
Hg13	1f	2/3	1/3	½	0.0090(4)	2/3	1/3	½	0.0157(7)
Hg14	1a	0	0	0	0.0162(5)	0	0	0	0.0222(8)

^a U_{eq} is defined as one-third of the trace of the orthogonalized U_{ij} tensor. ^b Statistical disorder of 0.96(1) Ca/0.04 Hg in $\text{Ca}_{10.92(2)}\text{Hg}_{54.08}$ and 0.74(2) Sr/0.26 Hg in $\text{Sr}_{10.48(4)}\text{Hg}_{54.52}$.

Table 4. Ranges of Interatomic Distances (Å) in $A_{11-x}\text{Hg}_{54+x}$ ($A = \text{Ca}, \text{Sr}$)

	$\text{Ca}_{10.92(2)}\text{Hg}_{54.08}$	$\text{Sr}_{10.48(4)}\text{Hg}_{54.52}$
A1–Hg	3.251(5)–3.405(6)	3.336(4)–3.521(6)
A2–Hg	3.221(2)–3.513(6)	3.332(2)–3.536(5)
A3–Hg	3.318(5)–3.511(7)	3.377(5)–3.549(6)
A4–Hg	3.200(2)–3.532(4)	3.265(2)–3.571(3)
A4–A4 ^a	3.766(1)	3.774(9)
Hg1–Hg	2.860(1)–3.649(2)	2.929(2)–3.770(2)
Hg2–Hg	2.853(1)–3.394(2)	2.896(2)–3.423(2)
Hg3–Hg	2.970(2)–3.649(2)	3.026(3)–3.770(2)
Hg4–Hg	2.921(1)–3.613(2)	2.974(2)–3.685(2)
Hg5–Hg	2.853(1)–3.820(2)	2.896(2)–3.759(3)
Hg6–Hg	2.860(1)–3.304(1)	2.929(2)–3.401(3)
Hg7–Hg	2.869(1)–3.489(2)	2.942(2)–3.759(3)
Hg8–Hg	2.995(2)–3.504(2)	3.056(2)–3.519(3)
Hg9–Hg	2.797(2)–3.337(2)	2.853(3)–3.332(3)
Hg10–Hg	2.797(2)–3.504(2)	2.853(3)–3.519(3)
Hg11–Hg	2.921(1)–3.300(2)	2.974(2)–3.292(3)
Hg12–Hg	2.910(2)–3.316(2)	2.951(2)–3.372(3)
Hg13–Hg	3.004(1)–3.300(2)	3.057(2)–3.292(3)
Hg14–Hg	2.995(2)–3.316(2)	3.052(2)–3.372(3)

^a A4 is a disordered site containing 0.96(1) Ca/0.04 Hg or 0.74(2) Sr/0.26 Hg.

in reciprocal space were carried out with an improved tetrahedron method over 28 irreducible k points.

Results and Discussion

Synthesis. Reactions of Ca or Sr with Hg conducted at 200 °C in increments of 5 at % in the Hg-rich regions (75–90%) of the A–Hg ($A = \text{Ca}, \text{Sr}$) systems showed that essentially single-phase products were obtained only at the nominal composition $A_{0.15}\text{Hg}_{0.85}$. This agrees well with the results obtained from the structure refinements, $A_{11-x}\text{Hg}_{54+x}$ (where $x < \sim 0.5$), which corresponds to the composition $A_{0.16}\text{Hg}_{0.84}$ and is significantly Hg-richer than previously believed ($A_{14}\text{Hg}_{51}$ or $A_{0.22}\text{Hg}_{0.78}$).^{2,3} Reactions deviating from this composition gave multiphase products containing Hg or SrHg_{11} in the Hg-richer reactions, and CaHg_3 or $\text{Sr}_{13}\text{Hg}_{58}$ in the Hg-poorer reactions, in the Ca–Hg and Sr–Hg systems, respectively. If substitutional disorder of A and Hg atoms within one site (A4) of the structure, as described below, is assumed to reach limiting extremes, the composition must be restricted to $A_{11}\text{Hg}_{54}$ ($x = 0$, or all A atoms in this site) at one end, and $A_9\text{Hg}_{56}$ ($x = 2$, or all Hg atoms in this site) at the other end. The maximum homogeneity range is thus less than 3 at % ($A_{11-x}\text{Hg}_{54+x}$ with $0 < x < 2$, or $A_{0.14-0.17}\text{Hg}_{0.86-0.83}$). The true homogeneity ranges are likely

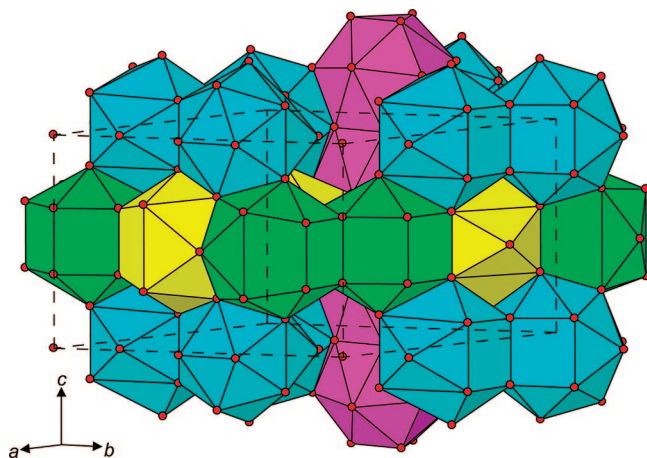


Figure 1. Structure of $A_{11-x}Hg_{54+x}$ in terms of polyhedra centered by the A sites: A1 (CN14, yellow), A2 (CN15, green), A3 (CN15, blue), A4 (CN16, magenta). Small red circles are Hg atoms.

narrower and will be different between the Ca and Sr systems. The powder X-ray diffraction patterns of the multiphase samples do show a detectable contraction in the refined cell parameters of $A_{11-x}Hg_{54+x}$ as A is substituted with smaller Hg atoms: $a = 13.446(1)–13.375(1)$ Å, $c = 9.661(1)–9.609(1)$ Å for the Ca system and $a = 13.730(1)–13.593(1)$ Å, $c = 9.927(1)–9.816(1)$ Å for the Sr system.

Structure. Like many other mercury intermetallics, the structure of $A_{11-x}Hg_{54+x}$ ($A = Ca, Sr$) is remarkably complex. Figure 1 shows a polyhedral representation in which four types of A-centered coordination polyhedra are densely packed to nearly occupy the entire unit cell. The remaining voids centered around the origin of the unit cell are occupied by Hg14 atoms. There are many crystallographically unique atoms (4 A and 14 Hg sites), some with quite irregular coordination geometries. Consistent with the larger sizes of A relative to Hg (metallic radii: Ca, 1.74 Å; Sr, 1.91 Å; Hg, 1.39 Å),²⁷ the A sites tend to have higher coordination numbers (CN14–16) (Figure 2) than do the Hg sites (CN11–13) (Figure 3). The coordination polyhedra around the A sites are well-defined, with the range of A–Hg distances (3.2–3.6 Å) not greatly exceeding the sum of the radii. However, the Hg–Hg interactions are more variable, with most distances (2.8–3.4 Å) that may be assumed to be significant in bonding, but with some longer distances seen up to a cutoff of 4.0 Å. To describe the structure in a simple way, a few longer distances, up to ~ 3.8 Å, have been included in defining the coordination geometries around the Hg sites. In this way, the coordination geometries fall into a manageable number of types.

Capped prisms characterize the polyhedra around A1 (tetracapped pentagonal prism, CN14), A2 (tricapped hexagonal prism, CN15), and A3 (pentacapped pentagonal prism, CN15), which are surrounded by Hg atoms only (Figure 2a). Hexagonal prisms are also found in $NaHg_2$ (AlB₂-type) with strictly parallel hexagonal faces²⁸ or in α -KHg₂ with buckled

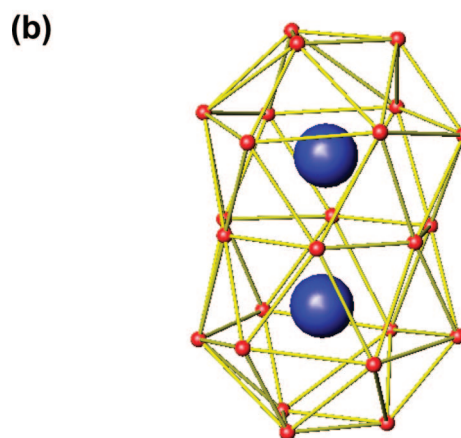
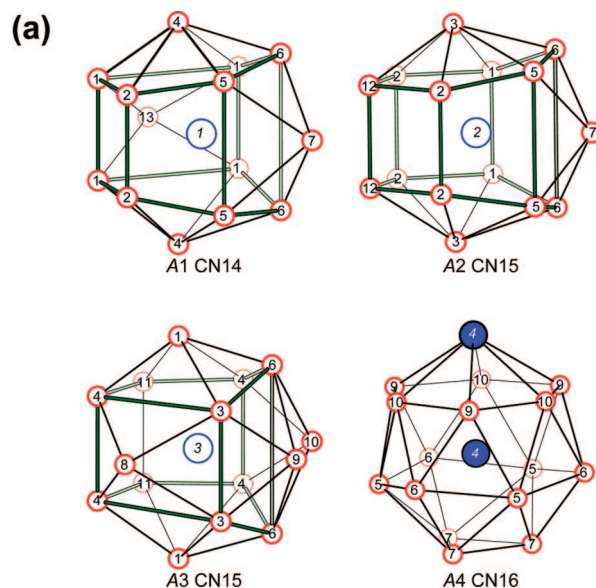


Figure 2. (a) Coordination polyhedra centered by A sites in $A_{11-x}Hg_{54+x}$, with a distance cutoff of 4.0 Å. A sites are blue, and Hg atoms are red. (A4 is a disordered site containing 0.96(1) Ca/0.04 Hg or 0.74(2) Sr/0.26 Hg.) (b) Interpenetrating Friauf polyhedra centered by A4 atoms in $A_{11-x}Hg_{54+x}$.

hexagonal faces²⁹ as is the case for the A2-centered polyhedron here. The A4 site differs in that it is subject to substitutional disorder (0.96(1) Ca/0.04 Hg in $Ca_{10.92(2)}Hg_{54.08}$; 0.74(2) Sr/0.26 Hg in $Sr_{10.48(4)}Hg_{54.52}$) and is centered in a Friauf polyhedron (CN16), which constitutes one of the Frank-Kasper polyhedra more typically found in intermetallic structures.³⁰ One of the vertices of this polyhedron is another A4 site, which brings two A4 sites close together, at a constant interatomic distance (3.77 Å for both $Ca_{11-x}Hg_{54+x}$ and $Sr_{11-x}Hg_{54+x}$). Although this distance is more than the sum of the metallic radii for Ca (3.48 Å), it is somewhat less than that for Sr (3.82 Å). This may explain why substitution of A with smaller Hg atoms in this site occurs to a greater extent in the Sr analogue. Two interpenetrating Friauf polyhedra can also be viewed as a pair of face-sharing CN15 polyhedra, forming an elongated cluster as shown in Figure 2b. These clusters are then arranged in columns aligned along the c direction, one of which may be seen,

(27) Pauling, L. *The Nature of the Chemical Bond*, 3rd ed.; Cornell University Press: Ithaca, NY, 1960.

(28) Nielsen, J. W.; Baenziger, N. C. *Acta Crystallogr.* **1954**, *7*, 277–282.

(29) Duwell, E. J.; Baenziger, N. C. *Acta Crystallogr.* **1955**, *8*, 705–710.

(30) Pearson, W. B. *The Crystal Chemistry and Physics of Metals and Alloys*; Wiley: New York, 1972.

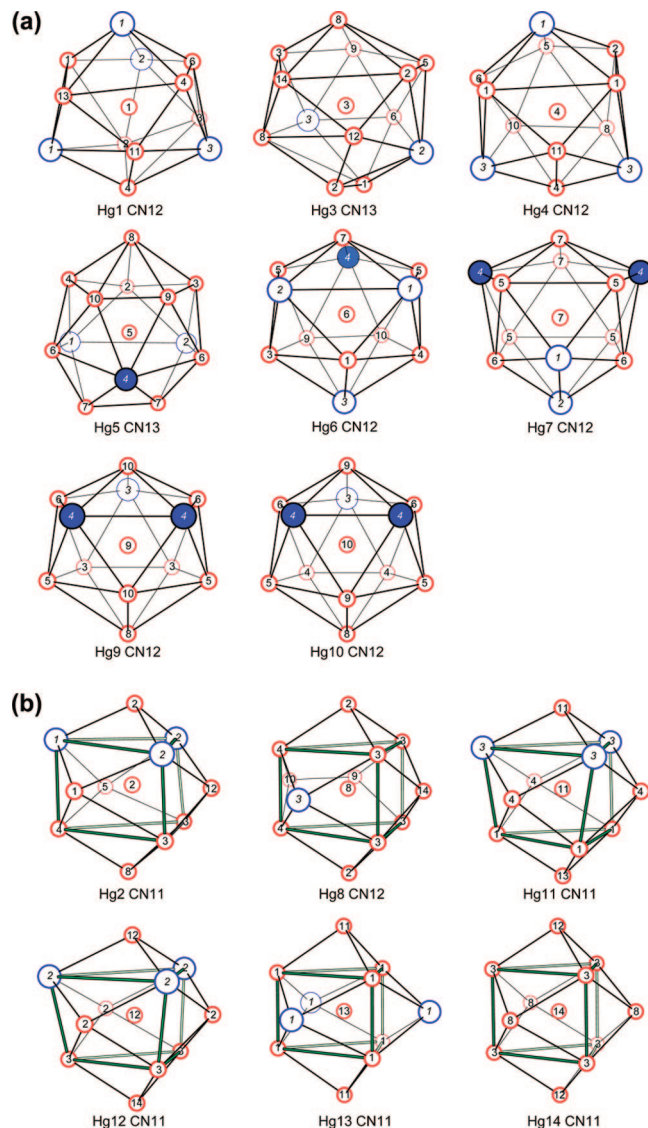


Figure 3. Coordination polyhedra centered by Hg sites in $A_{11-x}Hg_{54+x}$, with a distance cutoff of ~ 4.0 Å, derived from (a) icosahedra and (b) capped trigonal prisms. The color scheme is the same as in Figure 2a.

rendered in magenta and partially obscured, in Figure 1. Interestingly, similar columns are also found in K_7Hg_{31} (Ba_7Cd_{31} -type).³¹

In general, the Hg-centered coordination polyhedra may be grouped into two types: icosahedra (CN12) (Figure 3a) and pentacapped trigonal prisms (CN11) (Figure 3b). These are idealized descriptions as the true geometries are quite irregular. Although the icosahedra around Hg7, Hg9, and Hg10 possess at least a mirror plane, those around Hg1, Hg4, and Hg6 are severely distorted and lack any symmetry. The coordination around Hg3 and Hg5 is higher (CN13), but the geometry is closely related to an icosahedron if a corner atom is replaced by a pair of atoms. Except for the one around Hg2, the pentacapped trigonal prisms are more regular, with site symmetry 3 (Hg11, Hg12) or $\bar{6}$ (Hg13, Hg14). Similar pentacapped trigonal prisms are found in $NaHg_2$ (AlB_2 -type).²⁸ The higher coordination around Hg8 (CN12) results from replacing a capping atom with a pair of atoms.

(31) Todorov, E.; Sevov, S. C. *J. Solid State Chem.* **2000**, *149*, 419–427.

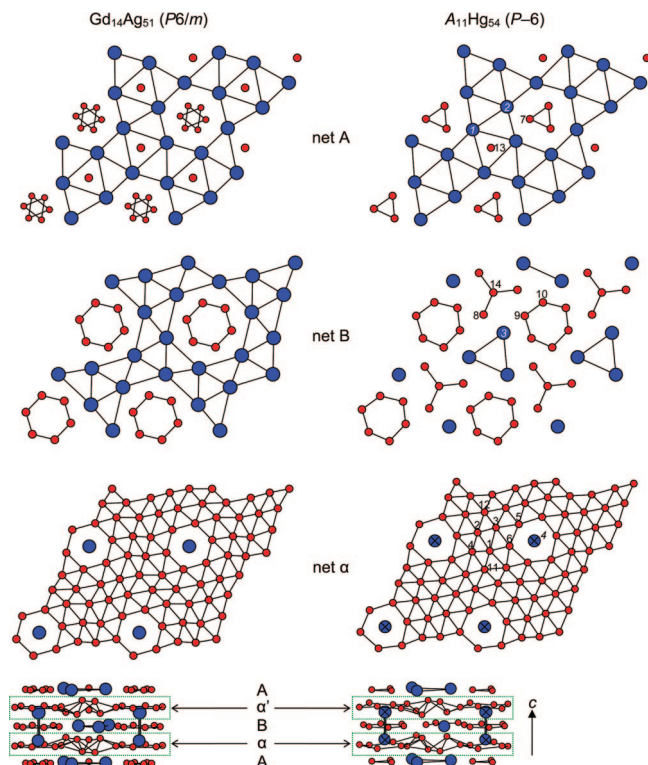


Figure 4. Comparison of $Gd_{14}Ag_{51}$ (left) and $A_{11-x}Hg_{54+x}$ (right) in terms of three different nets **A**, **B**, and α (viewed down the c direction, top three panels), stacked in the sequence $\alpha\alpha B\alpha'$ (thin sections viewed perpendicular to the c direction, bottom panel). Large blue circles are Gd or A atoms; small red circles are Ag or Hg atoms. See text for detailed explanation.

Many intermetallic structures can also be described in terms of a stacking of two-dimensional nets,³⁰ and accordingly, $A_{11-x}Hg_{54+x}$ ($A = Ca, Sr$) can be decomposed in this manner. As shown in Figure 4, this approach facilitates the comparison to the closely related $Gd_{14}Ag_{51}$ -type structure.⁴ Both are built up by alternately stacking primary nets **A** and **B**, which lie on $z = 0$ or $1/2$. These are then interleaved by secondary nets α (or α'), which lie on $z = 0.25 \pm 0.10$ (or $z = 0.75 \pm 0.10$). Net **A** consists of a triangular array of Gd or A atoms with large hexagonal voids. In $Gd_{14}Ag_{51}$, these voids contain a set of six symmetry-equivalent Ag sites that are half-occupied. Consideration of reasonable Ag–Ag separations leads to the conclusion that the Ag atoms cannot be distributed randomly within these sites; rather, the partial occupancy is interpreted as arising from disordered orientations of triangular Ag_3 clusters.^{4,19} (Very weak superstructure reflections have been reported for $Hf_{14}Cu_{51}$,¹⁵ associated with a doubling of the c axis, but no further study has been forthcoming.) In contrast, in $A_{11-x}Hg_{54+x}$, these voids now contain triangular Hg_3 clusters in ordered orientations, which can be resolved in the lower symmetry space group adopted. Additional single Ag atoms are embedded at the centers of some triangles in net **A** in $Gd_{14}Ag_{51}$, but the corresponding Hg atoms are only found within half of these triangles in $A_{11-x}Hg_{54+x}$. In $Gd_{14}Ag_{51}$, net **B** also consists of a triangular array of Gd atoms, but here, the hexagonal voids are large enough to accommodate planar hexagonal Ag_6 clusters. Similarly, in $A_{11-x}Hg_{54+x}$, planar hexagonal Hg_6 clusters are present, but there are also

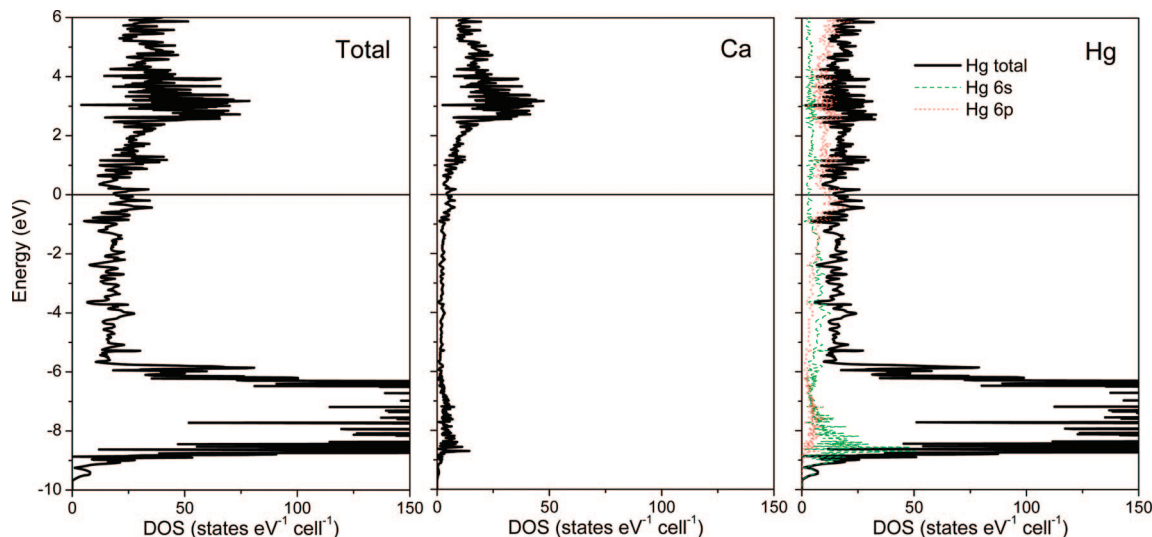


Figure 5. Total density of states (DOS) for $\text{Ca}_{11}\text{Hg}_{54}$ and its Ca and Hg projections. The Fermi level is marked by a horizontal line at 0 eV. In the right panel, the Hg 6s (green) and 6p (red) orbital contributions are also plotted.

centered trigonal planar Hg_4 clusters that substitute for points within the triangular array of net **B**. Although the nets α (or α') are highly buckled, they are easily seen to be triangular arrays as well. Single Gd or A4 sites occupy hexagonal voids within these arrays. The stacking of nets α and α' (above and below net **B**) creates Gd–Gd or A4–A4 pairs aligned along the *c* direction, which center the clusters of interpenetrating Friauf polyhedra described earlier.

Bonding. With relatively few electropositive *A* atoms available to transfer electrons to the more electronegative Hg atoms in $A_{11-x}\text{Hg}_{54+x}$, ionic character in the bonding will not be very pronounced. Several types of clusters, such as Hg_3 triangles and Hg_6 hexagons, were identified in the stacking description above, with Hg–Hg distances that are more characteristic of those in the elemental metal (3.00 Å)³² than in discrete molecules like Hg_2Cl_2 (2.526(6) Å).³³ Like other Hg-rich amalgams, these clusters really form part of a more extended three-dimensional network containing extensive Hg–Hg bonding. The density of states (DOS) derived from a band structure calculation on idealized $\text{Ca}_{11}\text{Hg}_{54}$ is shown in Figure 5. Consistent with calcium being cationic, most of the Ca 4s states are unoccupied, lying above the Fermi level, although there are still important contributions to the DOS below. The Hg 5d states are essentially completely filled, lying within a narrow range from –9 to –6 eV, whereas the Hg 6s and 6p states contribute to the DOS above –10 eV and beyond. The presence of occupied Hg 6p states supports the proposal of a partially anionic Hg substructure. With the caveat that charges derived from LMTO calculations are highly sensitive to the Wigner–Seitz radii of atoms, the average charges per atom were computed to be +0.34 for Ca and –0.07 for Hg, corresponding to the overall formulation $(\text{Ca}_{11})^{3.7+}(\text{Hg}_{54})^{3.7-}$. For comparison, negative charges between –0.1 and –0.3 were found for

the Hg atoms in $A_3\text{Hg}_{20}$ (*A* = Rb, Cs) from extended Hückel calculations.³¹

Conclusions

The structure of $A_{11-x}\text{Hg}_{54+x}$ (*A* = Ca, Sr) is somewhat different than originally proposed (Gd₁₄Ag₅₁-type) for the binary alkaline-earth metal mercury phases previously identified as $A\text{Hg}_{3.6}$.^{2,3} This suggests that the composition of related phases, such as “EuHg_{3.6}” and “YbHg_{3.6}”,¹⁶ should be re-evaluated. Assignment of the Gd₁₄Ag₅₁-type structure has normally been based solely on powder X-ray diffraction patterns, but subtle structural differences are more convincingly revealed from single-crystal X-ray diffraction, such as the presence of ordered triangular Hg_3 clusters. As noted previously for the Gd₁₄Ag₅₁-type,¹⁹ the structure of $A_{11-x}\text{Hg}_{54+x}$ is remarkable for the presence of more than four types of coordination polyhedra, a rare occurrence in binary intermetallic phases. A slight degree of electron transfer takes place from the *A* to Hg atoms to give a partially anionic “mercuride” substructure, consistent with the formulation $(\text{Ca}_{11})^{3.7+}(\text{Hg}_{54})^{3.7-}$, for example. However, size factors are also important in stabilizing this structure, as suggested by the variable homogeneity range associated with partial disorder of Hg atoms into one of the *A* sites.

Acknowledgment. The Natural Sciences and Engineering Research Council of Canada and the University of Alberta supported this work. We thank Dr. Robert McDonald and Dr. Michael J. Ferguson (X-ray Crystallography Laboratory) for the single-crystal X-ray data collection.

Supporting Information Available: X-ray crystallographic files in CIF format; tables listing Rietveld refinement results and selected interatomic distances; a figure summarizing Rietveld refinement results. This material is available free of charge via the Internet at <http://pubs.acs.org>.

IC7015148

(32) Donohue, J. *The Structures of the Elements*; Wiley: New York, 1974.

(33) Dorm, E. *J. Chem. Soc., Chem. Commun.* **1971**, 466–467.